Palm Shell Ash-based Geopolymer Mortar Innovation as a Sustainable Construction Solution

Andi YUSRA [1]*, Sanusi SANUSI [2], Fachruddin FACHRUDDIN [1]

[1] *Civil Engineering Department, Teuku Umar University, Meulaboh, Indonesia*
[2] *Technology and Informatics Department, Teuku Umar University, Meulaboh, Indonesia*

http://doi.org/10.5755/j02.ms.39657

Received 3 December 2024; accepted 14 August 2025

This study examines the potential use of palm shell ash, a byproduct of Indonesia's palm oil industry, as an environmentally sustainable alternative to cement in geopolymer mortar. The primary objective is to improve environmental sustainability by decreasing CO_2 emissions in the construction industry. The study utilizes an alkaline solution of sodium hydroxide (NaOH) and sodium silicate (Na_2SiO_3), along with silica fume and a superplasticizer, to assess the influence of palm shell ash on the mechanical, physical, and chemical properties of geopolymer mortar. Fourier Transform Infrared Spectroscopy (FTIR) to analyze functional group compounds, Scanning Electron Microscopy (SEM) for microstructure examination, and X-ray diffraction (XRD) to identify crystal phases. The work uses machine learning techniques to compare actual compressive strength with predicted values, aiming to enhance the accuracy of strength predictions. Initial findings suggest that using palm shell ash into geopolymer mortar improves mechanical performance and reduces reliance on conventional cement. This underscores the potential of palm shell ash as a sustainable material in the construction sector, contributing to environmental conservation and resource preservation.
Keywords: palm shell ash, geopolymer mortar, mechanical properties.

1. INTRODUCTION

Indonesia is the foremost global producer of palm oil, resulting in significant waste, including palm shells, which are frequently burnt or disposed of. Palm shells hold considerable promise as an industrial raw material, particularly to produce palm shell ash, which is abundant in silica and aluminium. This chemical is increasingly preferred by researchers as a precursor for the creation of environmentally sustainable building materials, including geopolymer mortar [1 – 4].

The growing demand for concrete in the construction sector has heightened the necessity for more environmentally sustainable alternatives to cement. Palm shell ash serves as a viable precursor for geopolymer, contributing to the reduction of industrial waste while exhibiting superior mechanical properties [5 – 8]. The amalgamation of palm shell ash with alkaline solutions, including sodium silicate and sodium hydroxide, has demonstrated the capacity to endow geopolymer materials with remarkable compressive strength and resilience against severe conditions.

While geopolymers produced with palm shell ash have demonstrated promising outcomes, the variability in the quality and strength of geopolymer mortar continues to be a significant concern. The ash's chemical composition, sintering temperature, and the ratio of alkaline solution are crucial elements that influence the final properties of the resulting geopolymer [7, 9 – 14]. Changes to the mechanical and physical characteristics of geopolymer mortar can be brought about by relatively small tweaks to these elements in many cases.

Research has demonstrated that utilizing palm shell ash as a precursor in geopolymer combinations can enhance compressive strength, chemical stability, and resistance to corrosive conditions [20 – 23]. The primary challenge in its application lies in stringent quality control and the optimization of production parameters, which may be affected by variations in the physical and chemical properties of the ash.

To examine the possibility of using palm shell ash, which is a byproduct of the palm oil industry in Indonesia, as an environmentally friendly replacement material for cement in geopolymer mortar, the goal of this research is to investigate the potential usage of palm shell ash. By reducing the amount of carbon dioxide emissions produced by the construction industry, the purpose of this study is to improve the environmental sustainability. In addition, the purpose of this study is to investigate the impact that palm shell ash has on the mechanical, physical, and chemical properties of geopolymer mortars, as well as to improve the accuracy of compressive strength prediction through the application of machine learning techniques. The use of palm shell ash, which is a plentiful byproduct of the palm oil industry, as an alternative to cement in the manufacturing of geopolymer mortar that is less harmful to the environment is what sets this study apart from others. This work also provides a novel method for forecasting the compressive strength of mortar, which has not previously been widely applied to geopolymer-based materials. This method was developed through the application of machine learning techniques. All these factors contribute to the sustainability of the building sector, and the study proposes viable strategies for reducing reliance on traditional cement,

* Corresponding author: A. Yusra
E-mail: *andiyusra@utu.ac.id*

lowering carbon emissions, and boosting resource efficiency.

2. RESEARCH METHODOLOGY

The palm shell ash used in this study is produced by incinerating palm shells into hard corals, which are then ground into a fine powder and sifted through a No. 200 sieve (Fig. 1). The palm oil processing company PT. SCOFINDO conducts this process. The palm shell ash serves as a precursor material, while silica fume (Table. 1) is included as an additional component. The diminutive particle size of palm shell ash, spanning from microns to submicron, enhances its reactivity in applications such as concrete or geopolymer mixtures. The material demonstrates a relatively low density compared to cement, leading to a reduction in the overall weight of construction materials when used as a binder.

Table 1. Chemical content in palm shell ash [8, 20 – 22]

Binder	Parameter test	Unit	Method	Result
Palm shell ash	SiO_2	%	Gravimetry	34.11
	$A1O_3$	%	Gravimetry	3.57
	Fe_2O_3	%	AAS	2.06
	SO_3	%	Titrimetric	0.2

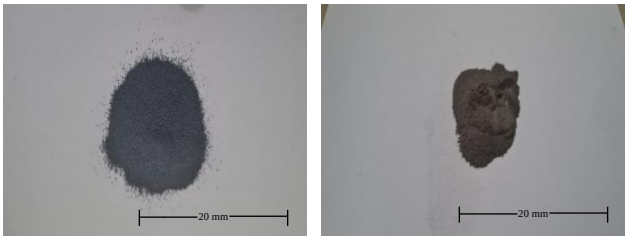

a B

Fig. 1. Silica fume used as a binder: a – additive; b – palm shell ash [4, 8, 12, 22, 23]

Palm shell ash's high porosity has a considerable impact on its water absorption and mechanical qualities when coupled with other materials like mortar. The typical blackish-gray tint is caused by residual carbon left over from the burning process, whereas lighter ash indicates a more complete combustion. The ash has a fine, smooth texture, allowing for easy integration with other materials. Furthermore, it contains minerals such as silica and alumina, as well as trace amounts of alkali metals and iron oxides. Palm shell ash is a suitable pozzolan material because of its high silica concentration, which improves the mechanical strength and chemical resistance of concrete [19].

This document specifies the physical standards for mortar, including grain size and the corresponding grain size distribution requirements. The activators employed in this process are sodium hydroxide (NaOH) and sodium sulphate ($NaSO_3$). The activator has been characterized as an alkaline solution. In the formulation of geopolymer mortar, different treatments were implemented using NaOH molarities of 6 M, 8 M, and 10 M, while $NaSO_3$ was consistently maintained at a molarity of 2.65 M. A total of 45 test specimens of geopolymer mortar are configured as prisms with dimensions of 50 mm × 50 mm × 50 mm. Fig. 2 illustrates the shape of the test piece along with the compressive strength test procedure as referenced by ASTM C109. Table 2 and Table 3 provide a detailed overview of the physical properties associated with fine aggregates.

This document specifies the physical standards for mortar, including grain size and the corresponding grain size distribution requirements. The activators employed in this process are sodium hydroxide (NaOH) and sodium sulphate ($NaSO_3$). The activator has been characterized as an alkaline solution. In the formulation of geopolymer mortar, different treatments were implemented using NaOH molarities of 6 M, 8 M, and 10 M, while $NaSO_3$ was consistently maintained at a molarity of 2.65 M. A total of 45 test specimens of geopolymer mortar are configured as prisms with dimensions of 50 mm × 50 mm × 50 mm. Fig. 2 illustrates the shape of the test piece along with the compressive strength test procedure as referenced by ASTM C109. Table 2 and Table 3 provide a detailed overview of the physical properties associated with fine aggregates.

Table 2. Specific gravity of fine sand

Aggregate type	Specific gravity		Reference
	SG (SSD)	SG (OD)	ASTM
Fine sand 0 – 2 mm	2.644	2.587	1.60 – 3.20

Table 3. Fine sand fineness modulus value

Aggregate type	Modulus fineness	Reference
Fine sand 0 – 2 mm	4.82	2.2 – 3.1

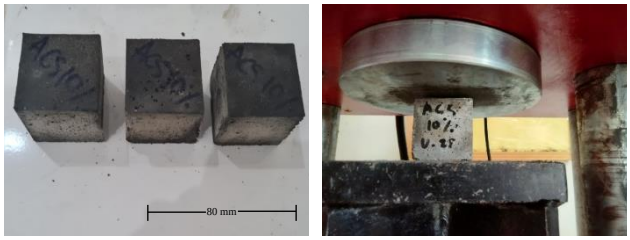

a b

Fig. 2. a – prism cube geopolymers mortar; b – specimen compressive strength

3. RESULTS

Table 4 presents detailed information regarding four variables: silica fume addition, NaOH molarity (M), NaOH ratio, and compressive strength in MPa. The average addition of silica fume was 10.00, with a standard deviation of 7.15, indicating significant variability within the dataset.

Table 4. Chemical elements based on general interpretation of XRD peaks

2Θ, degree	d-spacing, A	FWHM, °	Intensities, counts	Chemical elements
26.65	3.34	0.30	153	Si (Silica – SiO_2)
24.06	3.69	0.33	47	Al (Alumina – Al_2O_3), Si
29.44	3.03	0.25	38	Si (Silica – SiO_2)
21.95	4.04	0.40	36	Al (Alumina – Al_2O_3)
27.94	3.18	0.32	20	Si, Al (Silica alumina)

The distribution value of silica fume demonstrates a symmetrical pattern, with a minimum of 0 and a maximum of 20. The average molarity is recorded at 8.00, with a

standard deviation of 1.651, indicating a symmetrical distribution spanning from 6 to 10.

The ratio of NaOH to $NaSO_3$, averaging 0.72 with a standard deviation of 0.21, exhibits a distribution that is slightly right skewed. The ratio fluctuates between 0.50 and 1.00. The compressive strength value exhibits a notable variation, indicated by the measured average of 33.29 MPa alongside a standard deviation of 10.83 MPa. The distribution of compressive strength shows a nearly symmetrical pattern, with values spanning from a minimum of 14.91 MPa to a maximum of 54.82 MPa.

This table provides a comprehensive overview of the data distribution through various metrics, such as mean, median, mode, and measures of dispersion and skewness, including kurtosis, skewness, and standard deviation. This facilitates a comprehensive analysis of the patterns and distribution of data associated with each variable investigated in the experiment.

Fig. 3 presents the experimental results regarding the compressive strength of a 50 mm × 50 mm × 50 mm cube-shaped mortar geopolymer, highlighting the effects of varying NaOH molarity and differing amounts of silica fume addition.

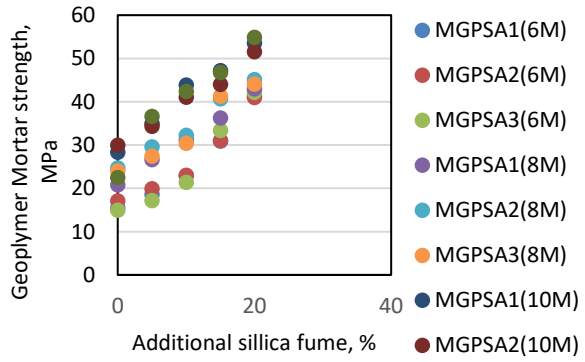

Fig. 3. Compressive strength of experimental geopolymer mortar based on palm shell ash with the addition of silica fume

The following review examines the compressive strength of geopolymer mortar in relation to variations in NaOH molarity, as illustrated in the graph. The compressive strength exhibits an increase with a higher percentage of silica fumes. The compressive strength of geopolymer mortar is positively correlated with the quantity of silica fume across all variations of NaOH molarity (6 M, 8 M, and 10 M). The average compressive strength at 0% fume silica ranges from 15 to 30 MPa. Incorporating up to 20 % silica fume can enhance the compressive strength to approximately 50 MPa, especially at elevated NaOH molarity.

Impact of NaOH Concentration, 6 M (MGPSA1, MGPSA2, MGPSA3): At a NaOH molarity of 6 M, the compressive strength of the geopolymer mortar increases, although it remains lower than that observed at higher molarities. The maximum compressive strength recorded at 20 % silica fume was approximately 40 – 45 MPa. At 8 M molarity, the compressive strength of geopolymer mortar (MGPSA1, MGPSA2, MGPSA3) exhibits a significant increase. The addition of 20 % silica fume results in an increase in compressive strength to approximately 50 MPa. This indicates that silica fume demonstrates significant efficacy at this molarity.

Conditions observed at 10 m (MGPSA1, MGPSA2, MGPSA3): The mortar's compressive strength peaks at 10 M molarity, approximately 50 MPa, and can approach 55 MPa with the inclusion of 20 % fume silica. This indicates that increased NaOH molarity enhances the influence of silica fume addition on compressive strength. The compressive strength of geopolymer mortars increases with higher NaOH molarity, reaching its peak at 10 M, in contrast to the strengths observed at 6 M and 8 M. The incorporation of up to 20 % silica fume significantly enhances the compressive strength of the mortar, especially at elevated NaOH molarities. Differences among groups: The compressive strength differential is minimal within each molarity group (MGPSA1, MGPSA2, MGPSA3), yet it increases with higher molarity and silica fume concentrations.

Fig. 4 displays the outcomes of a Scanning Electron Microscope (Thermoscientific Typen Prisma E Versi 16.0 made in USA) analysis on geopolymer mortar, illustrating its microstructure at a magnification of 1000×. The image depicts a complex, uneven, and porous surface characterized by various particle agglomerations, which manifest as lighter or darker regions based on their composition. The interconnected particles create a dense matrix that is essential for imparting mechanical strength to the geopolymer material.

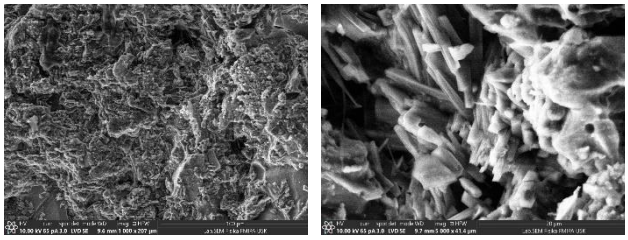

a b

Fig. 4. Microstructure of palm shell ash-based geopolymer mortar at optimum strength

A significant phase identified in the SEM image is the C-A-S-H (Calcium-Alumina-Silicate-Hydrate) compound. This phase develops as a secondary hydration product, like C-S-H in conventional cement, but incorporates alumina substitution. The C-A-S-H phase manifests as an amorphous or gel-like structure, frequently occupying pores and surrounding larger particles. The presence of this component significantly enhances the long-term strength and stability of the geopolymer mortar.

The quality and distribution of C-A-S-H compounds within the matrix are essential for mechanical properties such as compressive strength. A denser and more uniform C-A-S-H structure enhances mechanical performance. SEM images elucidate the influence of microstructure on mortar behaviour, revealing regions of effective particle bonding and C-A-S-H gel formation that improve load-bearing capacity. Nonetheless, the presence of small pores and cracks is evident, which could potentially diminish strength based on their prevalence.

Fig. 4 b displays the results of the SEM analysis, depicting the microstructure of the geopolymer material,

which consists of the components Al_2O_3 (alumina) and SiO_2 (silica). This image displays a unique and dense crystalline structure, highlighting improved details due to the extraordinary magnification of 5000×. The figure displays the results of the SEM analysis, depicting the microstructure of the geopolymer material, which consists of the compounds Al_2O_3 (alumina) and SiO_2 (silica). This image displays a crisp and dense crystalline structure, highlighting vivid details due to the exceptionally high magnification of 5000×.

The extensive crystalline structure depicted in the image is presumably the SiO_2 (silica)-rich phase. In geopolymer materials, silica constitutes a crystalline or amorphous phase and is pivotal in the formation of skeletal structures. Al_2O_3 molecules in geopolymers often function as fillers within silica frameworks, facilitating the formation of three-dimensional network structures that enhance the material's strength. Al_2O_3 may not be apparent in several crystalline forms; however, it is often associated with silica structures, forming aluminosilicate networks.

Multiple previous studies demonstrated that the SiO_2 phase in geopolymers tends to form either crystalline or amorphous structures, depending on the sintering temperature and basic content. The exhibited image corresponds with the characteristics outlined in previous studies, where the silica phase is clearly visible at high magnification, especially in the form of crystalline rods. Previous research has shown that increased Al_2O_3 content in geopolymer mixtures leads to the formation of denser aluminosilicate networks that display resistance to chemical degradation. This SEM image may illustrate a location where Al_2O_3 has interacted with SiO_2 to form this phase, although the alumina phase may not be easily discernible due to its common occurrence within a silicate matrix. The combination of Al_2O_3 and SiO_2 in geopolymer materials produces a highly stable and durable structure. The crystalline structure shown in the SEM image suggests that the material likely has considerable mechanical strength as a geopolymer mortar and demonstrates resistance to extreme environmental conditions, as documented. Fig. 5 illustrates that the numerous pores are evenly distributed, indicating that their effect on mechanical performance may be constrained if counterbalanced by well-formed C-A-S-H gels. The SEM images illustrate the intricate, multi-layered microstructure of geopolymer mortar, indicating that a dense C-A-S-H phase and reduced porosity enhance material performance. This analysis elucidates the influence of chemical composition and microstructure on the mechanical properties of geopolymers.

Fig. 5 illustrates the XRD data presented in the document, here is a thorough analysis of the results. The analytical measurement settings utilized an X-ray diffractometer (Merk Shimadzu XRD-7000 made in Japan) tube including a copper (Cu) target, functioning at a voltage of 40.0 kV and a current of 30.0 mA. The utilized slits comprised a 1.0° divergence slit, a 1.0° scatter slit, and a 0.3 mm reception slit. The scanning parameters varied from 10° to 80° Theta-2Theta in continuous scan mode, with a scanning velocity of 10°/min and a sample interval of 0.02°, accompanied by a predetermined duration of 0.12 seconds. The peak analysis indicates that the predominant phase in the sample corresponds to the peak at 26.65°, possibly signifying a primary crystalline constituent. Minor phases, denoted by peaks of reduced intensity, imply the existence of secondary constituents or contaminants.

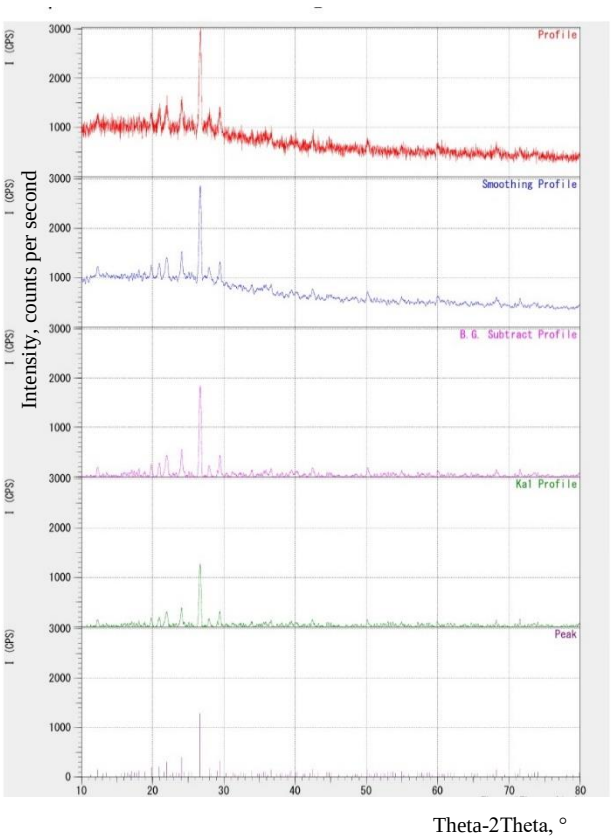

Fig. 5. XRD patterns of palm shell ash-based geopolymer mortar optimum strength

The Full Width at Half Maximum (FWHM) values elucidate the crystallinity of the sample, where diminished FWHM values signify larger, well-formed crystals, while elevated values denote smaller crystallites or lattice strain.

The sample's probable chemical makeup comprises silicon dioxide (SiO_2), which presumably accounts for the peaks at approximately 26.65° and 29.44°. Alumina (Al_2O_3) may correlate with the peak at 24.06°, influencing the mechanical characteristics of the sample. The existence of composite phases, including mixed oxides or silicates, is deduced from the overlapping or closely situated peaks reported by [46, 47].

To confirm the chemical composition and phases detected by XRD, further methods such as FTIR or SEM-EDS should be used. Analyzing the diffraction pattern alongside standard reference patterns from databases like ICDD can significantly improve the precision of phase identification. These guidelines seek to provide a more complete understanding of the sample's crystalline structure and composition [48, 49]. Table 4 shows the chemical compounds contained in the geopolymer mortar with optimum strength.

The most prominent three peaks recorded were at 2Theta values of 26.65°, 24.06°, and 29.44°. The peak at 26.65° had the maximum intensity, with an I/I1 ratio of 100 and an intensity of 153 counts, designating it as the most prominent

peak in the sample. Minor peaks were seen at several 2Theta values, including 21.95°, 27.94°, and 31.24°, exhibiting lower intensities between 10 and 36 counts.

Table 5 and Fig. 6 present the outcomes of the Fourier Transform Infrared Spectroscopy (FTIR) PerkinElmer made in USA analysis conducted on geopolymer mortar, highlighting the effects of varying silica fume additions at 5 %, 15 %, and 20 %. All geopolymer mortar samples exhibited a peak near 3467 cm^{-1}, which was identified as an alcohol characterized by hydrogen bonds (O–H stretching).

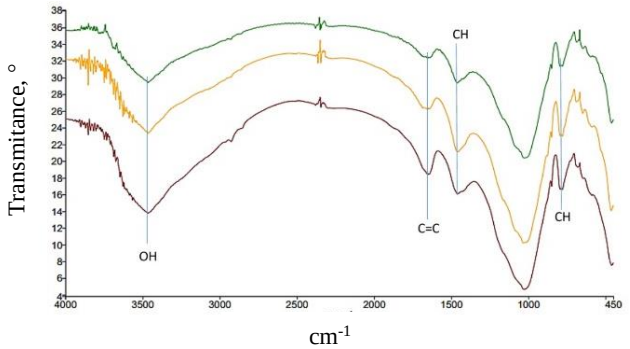

Fig. 6. Types of molecular bonds in MGPSA optimum strength

The observed peaks suggest the existence of hydroxyl groups (O–H), which play a role in the development of hydrogen bonds within the geopolymer structure as reported by [50 – 52]. The intensity of the geopolymer structure is subject to fluctuations that may arise from changes in water concentration or the conditions under which metal ions bind. The absorption peak observed in the range of 1646 – 1655 cm^{-1} corresponds to the presence of an alkene characterized by a carbon-carbon double bond (C=C Stretching). The existence of these bonds signifies the existence of unsaturated organic compounds within the sample. The intensity of these peaks exhibits variability, suggesting potential differences in the composition or distribution of organic compounds within geopolymers.

The absorption peak observed in the range of 1457 – 1459 cm^{-1} suggests the presence of alkane compounds characterized by C–H (C–H stretching) bonds. The strong intensity of these peaks indicates that the alkane compounds could potentially originate from organic residues or additives utilized during the production of geopolymer mortar [53 – 55]. The increase in silica fume concentration from 5 % to 20 % did not result in a notable shift in the position of the absorption peaks; however, the intensity of the peaks associated with C–H bonds remained robust, while those linked to O–H and C=C bonds exhibited variability.

4. CONCLUSIONS

In conclusion, the findings of the experiments are as follows:

Within the scope of this study, the compressive strength of geopolymer mortar is investigated in relation to the incorporation of silica fume and the utilization of varied molarities of NaOH. According to the findings of statistical study, the compressive strength of a material can be significantly improved by varying the amount of silica fume that is added by up to twenty percent and increasing the molarity of the sodium hydroxide from six to ten grams. The optimal results are achieved by combining 20 % silica fume with a molarity of 10 M sodium hydroxide, which results in a compressive strength of approximately 50 megapascals.

Tests of compressive strength have shown that increasing the molarity of sodium hydroxide (NaOH) in geopolymer mortar results in a constant increase in the compressive strength of the mortar. After six months, the compressive strength reaches between 40 and 45 MPa; however, after eight to ten months, when silica fume was incorporated into the mixture, the compressive strength increases to approximately 50 – 55 MPa. There is a significant increase in compressive strength when silica fume is present, particularly at significant concentrations.

Using scanning electron microscopy and X-ray diffraction, the microstructure analysis indicates the presence of the C-A-S-H phase. This phase is essential for providing the geopolymer with the necessary mechanical strength. The presence of major phases, such as silica (SiO_2) and alumina (Al_2O_3), which are connected with the chemical stability and mechanical integrity of the material, can also be detected by X-ray diffraction (XRD). Phase C-A-S-H plays a critical role in geopolymer matrices, markedly improving the mechanical strength and durability of the material. This phase reduces porosity and improves long-term stability, making it especially important in the application of geopolymer materials, particularly in adverse conditions.

Table 5. Compound function groups based on general interpretation of FTIR

Concentrate, %	Absorption area, cm^{-1}	Compound type	Bounds and types of functional group	Intensity
Sample mortar geopolymer add silica fume 5%	3467.67	Alcohols with hydrogen bonds	O–H stretching	Capricious
	1646.68	Alkene	C=C stretching	Capricious
	1458.76	Alkene	C–H stretching	Strong
	780.23	Alkene	C–H stretching	Strong
Sample mortar geopolymer add silica fume 15%	3467.84	Alcohols with hydrogen bonds	O–H stretching	Capricious
	1655.19	Alkene	C–C stretching	Capricious
	1459.03	Alkene	C–H stretching	Strong
	794.73	Alkene	C–H stretching	Strong
Sample mortar geopolymer add silica fume 20%	3467.86	Alcohols with hydrogen bonds	O–H stretching	Capricious
	1655.23	Alkene	C–C stretching	Capricious
	1457.95	Alkene	C–H stretching	Strong
	779.66	Alkene	C–H stretching	Strong

Acknowledgments

The authors would like to express their heartfelt gratitude to Universitas Teuku Umar for providing financial assistance through the internal research grant program. The Institute for Research and Community Service (LPPM) Universitas Teuku Umar supported this research under contract number 18/UN59.L1/AL.04/2025. We are also grateful to all colleagues and technical workers who assisted us in the accomplishment of this research. Their assistance and constructive feedback were critical to the success of our endeavour.

REFERENCES

1. **Abd Rahman, S.H. Farhan, S.A., Sazali, Y.A., Shafiee, L.H., Husna, N., Abd Hamid, A.l., Shafiq, N., Zulkarnain, N.N., Habaruddin, M.F.** Effect of Elastomeric Expandable Additive on Compressive Strength and Linear Expansion of Fly-Ash-Based Strength-Enhanced Geopolymer Cement for Shrinkage-Resistant Oil-Well Cementing *Applied Sciences* 12 (4) 2022: pp. 1897. https://doi.org/10.3390/app12041897
2. **Ahmed, Z.A.Z.E., Halim Naser, Y.N.A., Mohamed, H.A.S.V. R. A. S. G, Almasruri, M.A.N., Mohamed, R.A.S.G., Poloju, K.K.** Impact of Molarity on Compressive Strength of Geopolymer Conctrete *Journal of Student Research* 2021: pp. 1 – 11.
3. **Darwish, M., Khedr, S., Halim, F., Khalil, R.** Novel Simplified Construction of Walls and Prisms Made of CEBs and Earth-based Mortar *Practice Periodical on Structural Design and Construction* 25 (4) 2020: pp. 04020041. https://doi.org/10.1061/(ASCE)SC.1943-5576.0000525
4. **Zaimi, S.A., Halim, N.I., Sidek, M.N.M., Hashim, N.H.** Enhancement of Mortar Performance by Utilising POFA and GFRP as a Partially Replacement of Sand and Cement *Asian Journal of Fundamental and Applied Sciences* 4 (1) 2023: pp. 1 – 11. https://doi.org/10.55057/ajfas.2023.4.1.1
5. **Almadani, M., Razak, R.A., Abdullah, M.M.A.B., Mohamed, R.** Geopolymer-based Artificial Aggregates: A Review on Methods of Producing, Properties, and Improving Techniques *Materials* 15 (16) 2022: pp. 5516. https://doi.org/10.3390/ma15165516
6. **Ismail, A.H., Kusbiantoro, A., Tajunnisa, Y., Ekaputrc, J.J., Laory, I.** A Review of Aluminosilicate Sources from Inorganic Waste for Geopolymer Production: Sustainable Approach for Hydrocarbon Waste Disposal *Cleaner Materials* 2024: pp. 100259. https://doi.org/10.1016/j.clema.2024.100259
7. **Luhar, I., Luhar, S.** A Comprehensive Review on Fly Ash-based Geopolymer *Journal of Composites Science* 6 (8) 2022: pp. 219. https://doi.org/10.3390/jcs6080219
8. **Qaidi, S., Najm, H.M., Abed, S.M., Ahmed, H.U., Al Dughaisi, H., Al Lawati, J., Sabri, M.M., Alkhatib, F., Milad, A.** Fly Ash-based Geopolymer Composites: A Review of the Compressive Strength and Microstructure Analysis *Materials* 15 (20) 2022: pp. 7098. https://doi.org/10.3390/ma15207098
9. **Balçikanli Özbay, M., Türker, E.H.T., Karahan, O., Atiş, C.D.** Optimum Design of Alkali Activated Slag Concretes for Low Chloride Ion Permeability and Water Absorption Capacity *International Journal of Structural and Construction Engineering* 10 (11) 2017: pp. 1474 – 1477. http://scholar.waset.org/1307-6892/10007382
10. **Hassan, A., Arif, M., Shariq, M.** Use of Geopolymer Concrete for a Cleaner and Sustainable Environment–A Review of Mechanical Properties and Microstructure *Journal of Cleaner Production* 223 2019: pp. 704 – 728. https://doi.org/10.1016/j.jclepro.2019.03.051
11. **Moukannaa, S., Nazari, A., Bagheri, A., Loutou, M., Sanjayan, J.G., Hakkou, R.** Alkaline Fsed Phosphate Mine Tailings for Geopolymer Mortar Synthesis: Thermal Stability, Mechanical and Microstructural Properties *Journal of Non-Crystalline Solids* 511 2019: pp. 76 – 85. https://doi.org/10.1016/j.jnoncrysol.2018.12.031
12. **Mustapa, N.B., Ahmad, R., Ibrahim, W.M.W, Al-Bakri Abdullah, M.M., Wattanasakulpong, N., Nemeş, O., Sandu, A.V., Vizureanu, P., Sandu, I.G., Kartikowati, C.W., Risdanareni, P.** Effect of Sintering Mechanism towards Crystallization of Geopolymer Ceramic – A Review *Materials* 16 (11) 2023: pp. 4103. https://doi.org/10.3390/ma16114103
13. **Özbayrak, A., Kucukgoncu, H., Aslanbay, H.H., Aslanbay, Y.G., Atas, O.** Comprehensive Experimental Analysis of the Effects of Elevated Temperatures in Geopolymer Concretes with Variable Alkali Activator Ratios *Journal of Building Engineering* 68 2023: pp. 106108. https://doi.org/10.1016/j.jobe.2023.106108
14. **Zhuang, X.Y., Chen, L., Komarneni, S., Zhou, C.H., Tong, D.S., Yang, H.M., Yu, W.H., Wang, H.** Fly Ash-based Geopolymer: Clean Production, Properties and Applications *Journal of Cleaner Production* 125 2016: pp. 253 – 267. https://doi.org/10.1016/j.jclepro.2016.03.019
15. **Ahmad, S., Al-Amoudi, O.S.B., Khan, S.M., Maslehuddin, M.** Effect of Silica Fume Inclusion on the Strength, Shrinkage and Durability Characteristics of Natural Pozzolan-based Cement Concrete *Case Studies in Construction Materials* 17 2022: pp. e01255. https://doi.org/10.1016/j.cscm.2022.e01255
16. **Handayani, L. Aprilia, S., Abdullah Rahmawati, C., Aulia, T.B., Ludvig, P., Ahmad, J.** Sodium Silicate From Rice Husk Ash and Their Effects as Geopolymer Cement *Polymers* 14 (14) 2022: pp. 1 – 14. https://doi.org/10.3390/polym14142920
17. **Rizzuti, A.** Organized Crime in the Agri-food Industry *In The Private Sector and Organized Crime* 2022: pp. 163 – 179.
18. **Vaïmata, G.D., Djakba, R., Dobe, N., Madibalo, A., Kaze, R.C., Boughzala, H., Massai, H.** The Effect of Combining Rice Husk Ash with Laterite-based Inorganic Polymers Activated by Potassium-rich Shea Pellet Ash *Sustainable Chemistry and Pharmacy* 39 2024: pp. 101607. https://doi.org/10.1016/j.scp.2024.101607
19. **Hasan, K., Yahaya, F.M., Karim, A., Othman, R.** Investigation on the Properties of Mortar Containing Palm Oil Fuel Ash and Seashell Powder as Partial Cement Replacement *Construction* 1 (2) 2021: pp. 50 – 61. https://doi.org/10.15282/construction.v1i2.6679
20. **Yusra, A.** Effect of Additive Variations on the Mechanical Properties of High-Quality Concrete. Universitas Syiah Kuala, Aceh, 2014.
21. **Ikubanni, P.P., Oki, M., Adeleke, A.A., Adediran, A.A., Adesina, O.S.** Influence of Temperature on the Chemical Compositions and Microstructural Changes of Ash Formed from Palm Kernel Shell *Results in Engineering* 8 2020: pp. 100173.

22. **Rasid, N.N.A., Khalid, N.H.A., Mohamed, A., Sam, A.R.M., Majid, Z.A., Huseien, G.F.** Ground Palm Oil Fuel Ash and Calcined Eggshell Powder as SiO2–CaO Based Accelerator in Green Concrete *Journal of Building Engineering* 65 2023: pp. 105617.
23. **Yusra, A., Hasan, M., Husin, H., Aulia, T.B.** The Impact of Silica Fume Addition on the Early Age Compressive and Flexural Strength of Geopolymer Mortar with Various Binders *E3S Web Conference* 621 2025: pp. 01007. ttps://doi.org/10.1051/e3sconf/202562101007
24. **Bañuelos, J.L., Borguet, E., Brown, Jr.G.E., Cygan, R.T., DeYoreo, J.J., Dove, P.M., Gaigeot, M.P., Geiger, F.M., Bañuelos, J.L., Grassian, V.H., Ilgen, A.G., Jun, Y.S., Kabengi, N., Katz, L., Kubicki, J.D., Lützenkirchen, J., Putnis, C.V., Remsing, R.C., Rosso, K.M., Rother, G., Sulpizi, M., Villalobos, M., Zhang, H.** Oxide–and Silicate–water Interfaces and their Roles in Technology and the Environment *Chemical Reviews* 123 (10) 2023: pp. 6413 – 6544. https://doi.org/10.1021/acs.chemrev.2c00130
25. **Polavaram, K.C., Garg, N.** Enabling Phase Quantification of Anhydrous Cements via Raman Imaging *Cement and Concrete Research* 150 2021: pp. 106592. https://doi.org/10.1016/j.cemconres.2021.106592
26. **Holder, C.F., Schaak, R.E.** Tutorial on Powder X-ray Diffraction for Characterizing Nanoscale Materials 13 (7) *ACS Publications* 2019: pp. 7359 – 7365. https://doi.org/10.1021/acsnano.9b05157
27. **Karimi, K., Taherzadeh, M.J.** A Critical Review of Analytical Methods in Pretreatment of Lignocelluloses: Composition, Imaging, and Crystallinity *Bioresource Technology* 200 2016: pp. 1008 – 1018. https://doi.org/10.1016/j.biortech.2015.11.022
28. **Rees, C.A., Provis, J.L., Lukey, G.C., Van Deventer, J.S.** In Situ ATR-FTIR Study of the Early Stages of Fly Ash Geopolymer Gel Formation *Langmuir* 23 (17) 2007: pp. 9076 – 9082. https://doi.org/10.1021/la701185g
29. **She, Y., Chen, Y., Li, L., Xue, L., Yu, Q.** Understanding the Generation and Evolution of Hydrophobicity of Silane Modified Fly Ash/slag Based Geopolymers *Cement and Concrete Composites* 142 2023: pp. 105206. https://doi.org/10.1016/j.cemconcomp.2023.105206
30. **Zhang, W., Dong, C., Huang, P., Sun, Q., Sun Li, M., Chai, J.** Experimental Study on the Characteristics of Activated Coal Gangue and Coal Gangue-based Geopolymer *Energies* 13 (10) 2020: pp. 2504. https://doi.org/10.3390/en13102504
31. **Kankia, M.U., Baloo, L., Danlami, N., Mohammed, B., Haruna, S., Abubakar, M., Jagaba, A.H., Sayed, K., Abdulkadir, I., Salihi, I.U.** Performance of Fly Ash-based Inorganic Polymer Mortar with Petroleum Sludge Ash *Polymers* 13 (23) 2021: pp. 4143. https://doi.org/10.3390/polym13234143
32. **Reeb, C., Pierlot, C., Davy, C., Lambertin, D.** Incorporation of Organic Liquids into Geopolymer Materials-A Review of Processing, Properties and Applications *Ceramics International* 47 (6) 2021: pp. 7369 – 7385. https://doi.org/10.1016/j.ceramint.2020.11.239
33. **Shill, S.K., Al-Deen, S., Ashraf, M., Hutchison, W.** Resistance of Fly Ash Based Geopolymer Mortar to Both Chemicals and High Thermal Cycles Simultaneously *Construction and Building Materials* 239 2020: pp. 117886. https://doi.org/10.1016/j.conbuildmat.2019.117886